Characterization of collagen/lipid nanoparticle-curcumin cryostructurates for wound healing applications

Valentina Laghezza Masci[1], Anna-Rita Taddei[2], Thomas Courant[3], Ozgül Tezgel,[3]Fabrice Navarro[3], Franco Giorgi[4], Denis Mariolle[3],Anna-Maria Fausto[1], Isabelle Texier[3*]

[1] Department for Innovation in Biological, Agrifood and Forestry Systems (DIBAF), Tuscia University, Italy

[2]Section of Electron Microscopy, Tuscia University, Italy

[3] Univ. Grenoble Alpes, CEA, LETI, F-38000 Grenoble, France

[4] University of Pisa, Italy

Abstract

Curcumin-loaded collagen cryostructurateshavebeen devised for wound healing applications. Curcumin displays strong antioxidant, antiseptic, and anti-inflammatory properties, while collagen is acknowledged for promoting cell adhesion, migration and differentiation. However, when curcumin was loaded directly into collagen hydrogels, it formed large molecular aggregates and clogged the matrix pores.A double encapsulation strategy wastherefore developed by loading curcumin into lipid nanoparticles (LNP), and embedding these particlesinside collagen scaffolds. The resulting collagen/LNP cryostructurateshavean optimalfibrous structure with ≈100 µm average pore size for sustaining cell migration. Results showed that collagen was structurally unaltered and that nanoparticles were homogeneously distributedamidst collagen fibers. Hydrogels soaked in saline buffer released about 20% to 30% of their nanoparticles content within 24h, while achieved 100 % release after 25 days.When exposed to NIH 3T3 fibroblasts, these hydrogels provided a satisfactory scaffold for cell interaction as early as 4 h after seeding with no cytotoxic counter effect. These positive features make the collagen/lipid cryostructurates a promising material for further use in wound healing.

Keywords

Collagen ; curcumin ; lipid nanoparticles ; wound healing ; SEM ; TEM ; AFM

Graphical abstract

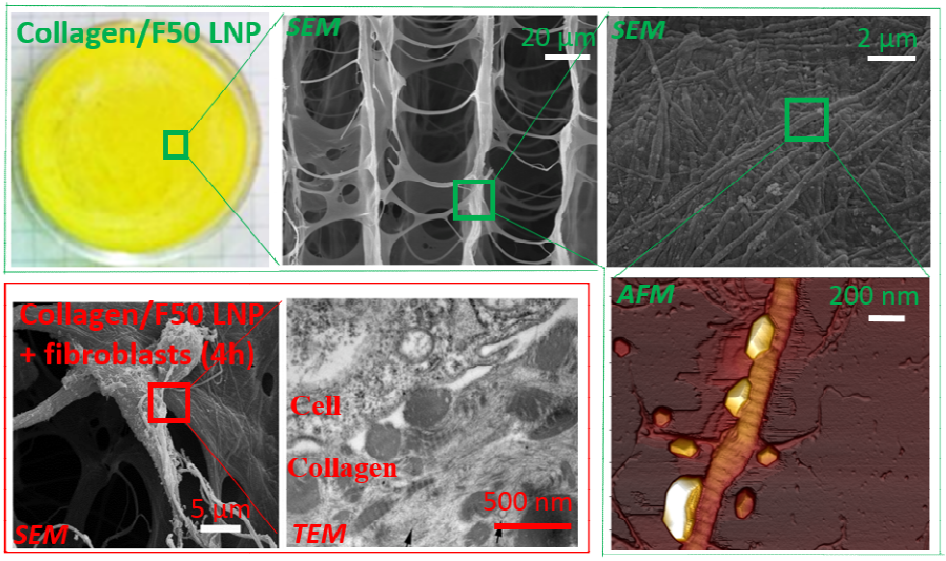

Short summary

Curcumin-loaded lipid nanoparticles (LNP) were loaded into collagen cryostructuratesto design innovative wound healing materials. The collagen/LNP scaffolds were characterized by different techniques (SEM, TEM, AFM, DSC, compression…) to assess their structural and mechanical properties. They displayed good adhesion properties with both keratinocytes and fibroblasts, and double encapsulation strategy prolonged curcumin payload release.

Introduction

For a wound to heal successfully, several cellular and molecular mechanisms have to act in a proper temporal sequence.[1-2] Improper healing causes the wound to enter an intransigent phase of chronicity, due to a high severity score of the injury itself or to a low health state of the patient. For instance, the fast growing incidence of diabetes mellitus expose many patients at the risk of developingsuch a chronic non-healing complication as foot ulcer.[2]In these conditions, high concentrations of proteases, reactive oxygen species, senescent cells and impaired stem cells are all hallmarks of chronic wounds.[1]

In recent years, artificial scaffoldingsacting as skin substitutes have been developed to improve wound healing.[1-2]Because of its relative abundance in bodily proteins, its structural role as a main component of the extracellular matrix, its low immunogenicity and high stability, collagen is *par excellence* the best biomaterial to be employed as a prosthetic medical device for wound healing, except for patients prone to keloid scaring, for whom collagen deposition in the wound bed is excessive.[3-4]Collagen ismade by the self-assembly and binding of tropocollagen molecules, composed of three helical polypeptide chains wound around each other to form a triple helix. The resulting fiber acts as a stable scaffold for cell attachment by means of numerous RGD integrin-binding motifs.Collagen is also known to play important roles in cell migration and differentiation, by counteracting elevated concentrations of metalloproteases, and eventually enhancinggranulation tissues and neo-angiogenesis.[5] Different collagen materials have been proposed for wound healing purposes, based on pure collagen [5]or combined with other biocompatible polymers, such as alginate,[6] chitosan,[7] or cellulose.[8]However, the adoption of aggressive extraction and processing proceduresmay denature collagenand modifyits structuraland chemotactic properties[5]. In a previous study,a few commercial collagen-based materials were compared toevaluate howcells and matrix interact in relationto pore sizes, mechanical stability and susceptibility to

proteolytic degradation.[9]The best structural conditions were provided by native collagencryostructuratesobtained by freeze-drying of 1% w/v collagen gel in acetic acid, characterized by high matrix porosity and thick fiber bundles.[9] Under these conditions, cells proliferated, migrated and adhered to the collagen fibers through extended filopodia.[10-11]

Several therapeutic strategies have recently been proposed to complement these scaffold features with antimicrobial or wound-healing promoting properties[12-13].For instance, silver nanoparticles have been included in different commercial products (Acticoat®, Smith & Nephew; Altreet® Ag, Coloplast; Urgotuls Ag®, Urgo). In this study, we focused on the polyphenol curcumin which has been widely used for centuries in the traditional medicines of China and India. Curcumin exhibitssome antimicrobial, antioxidant, antiseptic and anti-inflammatory properties, besides expressing a potential MMP inhibiting activity,[14-15] and has recently aroused much interest for wound healing applications.[16-17] It has also been demonstrated to accelerate wound healing via different biological processes, such as regulation of cytokine levels and MMP9 concentration in wound beds. Together, these factors enhance tissuegranulationthrough fibroblast proliferation, help to deposit new collagen, stimulate neo-angiogenesis and regenerate epithelial layers.[16-17]

New collagen/curcumin cryostructurateswere therefore designedwith the intentof preservingallmajor hallmarks of collagen matrix for wound healing, i.e. high microporosity, convenientswelling ratio, goodmechanical properties and favorable conditions for cell interaction. Since direct curcumin loading in the collagen matrix occluded the cryostructuratepores, we show here that loading the drug in lipid nanoparticles (LNP)embedded in the cryostructurate preserved all properties of the collagen scaffold.

Several physico-chemical analyses have also been carried out to check how properties of these cryostructuratescompared to those of pure collagen scaffolds. Structural interactions

with fibroblasts havealso been assessed by Scanning Electron Microscopy (SEM) and Transmission Electron Microscopy (TEM).

2. Results and discussion

2.1. Preparation of curcumin-loaded collagen cryostructurates

In this study, collagen type I extracted from equine Achilles tendon and dispersed in 1% w/v acetic acid at pH 3was employed to obtain cryostructurates by freeze-drying. Collagencryostructuratesare known to absorb large amount of wound exudate andmaintain a moist environment in the wound.[3-5]

In a first experimental design, curcumin was dissolved in small volumes of ethanol and mixed with the collagen gel,and the resulting slurry gently stirred to ensure complete homogenization before freeze-drying (**Figure 1**A). However, when observed by SEM, the resulting matrix did not display theusual aspectsof payload-free collagen, some pores appearing obstructed by curcumin aggregates (Figure 1B).[10]

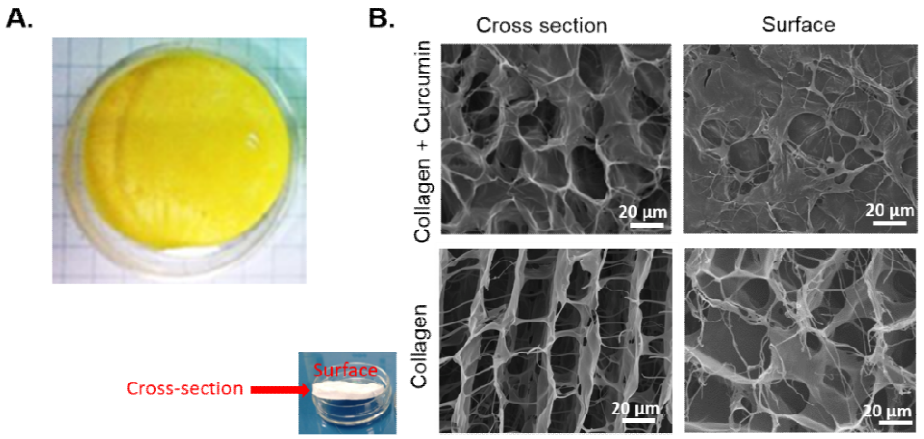

Figure 1. Collagen cryostructuratesprepared by direct curcumin loading (1 mg curcumin/g collagen). **A.** Photograph of the collagen scaffold. **B.**SEM images of collagen cryostructurates loaded with curcumin (top) and compared with pure collagen cryostructurates (bottom).

Curcumin is acknowledged for itslow solubility and high chemical degradation rate in aqueous environment, along with low tissue absorption and short plasma life-time. These properties make its formulation for wound healing applications a challenging task.[18]For loading curcumin in hydrogel scaffolds, several “double-encapsulation”strategies have been recently proposed. They all rely on the experimental formulation of curcumin-loaded polymer microparticles,[8] nanoparticles,[6]ornanomicelles,[19-22]that are themselves encapsulated inside the hydrogel matrix. For instance, curcumin-loaded gelatin microspheres measuring a few micrometer in diameter were loaded in collagen-cellulose nanocrystal scaffolds,[8]and 200 nm diameter drug-encapsulatedchitosannanoparticles were incorporated in collagen-alginate scaffolds.[6]

In this study, curcumin was encapsulated in lipid nanoparticles (LNP). LNP are core-shell particles made of human-used approved ingredients, produced by up-scalable solvent-free high pressurehomogenization. Theycan be used as stable non-toxic carriers for water-insoluble drugs or fluorescent molecular probes.[23-24] These particleshave been shown to act as drug reservoirs for the stratum corneum both in intact and damaged skin,[25-26]and loaded with morphine or other opioids,[27]astragaloside IV,[28]antimicrobial peptides,[29]orvarying growth factors[30]for wound healing purpose. Preliminary reports indicate that their lipid core may play positive roles in wound healing[27, 31-33]by affecting the penetration rate of the encapsulated drugs[26].

Thedouble encapsulation technology developed in this study entails first curcumin entrapment into lipid nanoparticles followed bytheir uploading into collagen matrix (**Figure 2**A). Curcumin-loaded lipid nanoparticles with hydrodynamic diameters of 50 nm (F50) or 120 nm (F120) were synthesized using previously described protocols.[34-35] Theirmain featuresare summarized in Figure 2B. The particle hydrodynamic diameters were adjusted by regulating the lipid and surfactant ratios.[36]Encapsulation efficiency andfinal payload were

higher for F120 than for F50 (Figure 2B), due to their higher lipid/surfactantratioand larger drug loading volume. F50 and F120were then homogeneously dispersed in a collagen gel (collagen/lipid particle 10/1 w/w) by gentle stirring for about one hour, and the resulting slurry freeze-dried to produce a structurally uniform collagen matrix, as assessed by SEM (Figure 2C).The presence of nanoparticlesof about 100 nm and 180 nm in diameter, for collagen/F50 and collagen/F120 samplesrespectively, could be envisionedby high resolution SEM (Figure 2C). At low magnification, collagen fibers are characterized by a trabecular pattern of vertically oriented laminas connected by thin filaments, as it is usual for collagen matrices.[10]This organization remained invariant following nanoparticle addition(collagen/lipid ratio of 10/1 w/w), unlike encapsulation of chondroitin sulfate liposomes that was shown to cause an increase incollagen pore sizes in studies on osteoarthritis.[37]

Pore sizes of the collagen/LNPcryostructurateswere measured directly by SEM using the ImageJ® software, and results are summarized in **Table 1**.All cryostructurates, regardless of nanoparticle presence, displayedanaverage pore size of 80-100 μm, as previously reported.[38-39]A pore size of about 50-150 μmis anoptimalmeasure for sustaining cell migration in collagen matrices.[38, 40]Collagen cryostructurateswith high porosity provide healthy healing environment by facilitatingdiffusion of nutrients and oxygen, and absorbing exudate fluids and blood.[10]Increase in lipid nanoparticlesmade the collagen matrix progressively more irregular, particularly if the collagen/lipid ratio is below 3.3/1 (Supporting Information Figure S1).The Feret's diameter was measured in collagen matrices differing in particle payloads. Data show that pore sizes remained invariant for up to very high collagen/lipid 2.5/1 ratio (Supporting Information Table S1), while started to increase for collagen/lipid ratios close to 2/1 (Table S1). This is in line with data from Atomic Force Microscopy (AFM) on hydrated samples showingthatthe collagen matrixbecame progressively more destructured for high

particle payloads (Supplementary Information, Figure S2). Therefore, unless otherwise specified,data presented in the following sections refer tocryostructuratesmade with collagen/lipid ratios of 10/1 w/w.

A.

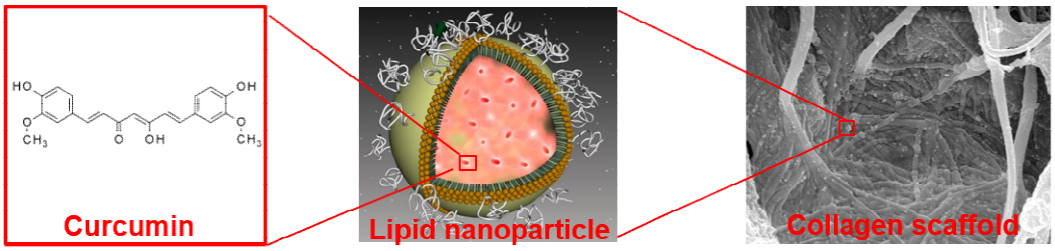

B.

	F50	F120
Hydrodynamic diameter (nm)	59.7 ± 1.1 nm	119.7 ± 1.2 nm
Polydispersity index	0.19 ± 0.01	0.15 ± 0.01
Curcumin encapsulation yield (%)	51 ± 2 %	92 ± 4 %
Stability	> 5 months, 4°C	> 5 months, 4°C

C.

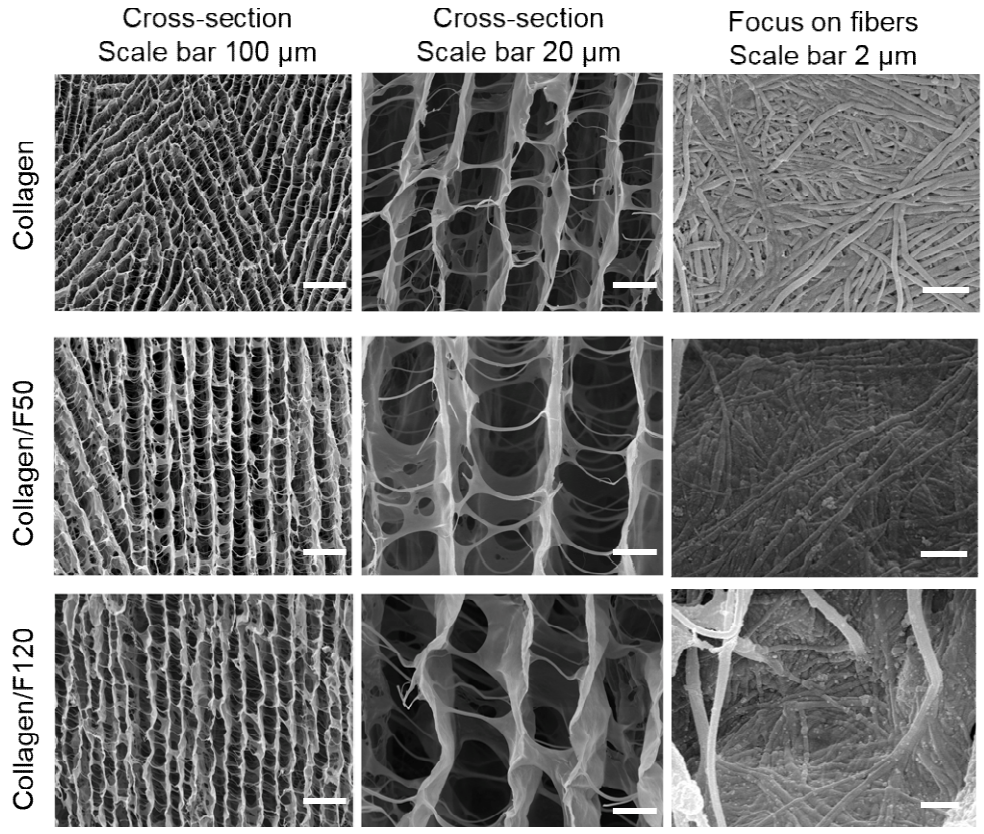

Figure 2. Cryostructurates with doubly-encapsulated curcumin. **A.** Principle of double-encapsulating material. **B.** Properties of curcumin-loaded lipid nanoparticles. **C.** SEM images

ofcollagen versus collagen/lipid cryostructurates for two different lipid nanoparticles (F50, F120).

2.2. Lipid particle distribution in cryostructuratesand material stability

To ascertainhow lipid nanoparticleswere distributed in collagen matrices, DiI and DiDfluorescent lipophilic tracers were loaded within LNP in a 1:4 ratio. LNPintegrityand stability were then monitored by Fluorescence Resonance Energy Transfer (FRET).[41]

FRET-labeled nanoparticles remained stable for about 24 hours in the collagen slurry, a time lapse sufficient for the subsequent gel freezing process (Supporting Information Figure S3). LNP distribution was then assessed by confocal laser scanning microscopy (CLSM) (Supporting Information, Figure S4). Under these conditions,DiI and DiDfluorescent signalsappeared constant all over the collagen matrix, indicating that nanoparticles were uniformly dispersed and firmly embedded amongst the collagen fibers.

To assess the extent of particle stability in cryostructuratesin ambient atmosphere, nanoparticles were extracted from the collagen scaffold andexamined at varying time-lapses following storage (**Figure 3**A). Both nanoparticle diameter (Figure 3B) and polydispersity index (Figure 3C) were measured by Dynamic Light Scattering (DLS). Data show that, when analyzed after collagen embedment and collagenase digestion (t=0), both F50 and F120 nanoparticles exhibited a mean size of about 170 nm and a polydispersity index around 0.25 (Figure 3B,C). These values were higher than those detectable in solution before LNP insertion (Figure 2B), but close to the ones exhibited after collagen gel mixing (Supporting Information, Figure S3). Nanoparticle sizes measured by SEM (Figure 2) didalso indicate

larger values in cryostructuratesthan in solution, a condition likely to depend upon the collagen absorption on the particle surface following gel digestion by collagenase.

However,particle size and polydispersity index remained invariantfor the following 100 days (Figures 3B, 3C), indicatinga remarkable particlestability. **Figure 3D**showsthe particle FRET signal, resultingfrom the stability of DiI/DiD encapsulation and hence from the integrity of the particle core. The FRET signal was reduced by about ≈ 10% and ≈ 40 % for F50 and F120,respectively, soon after cryostructurate preparation (t=0). This indicates that some particles may have either leaked or disintegrated during preparation. The observation of a similar FRET signal decrease 24 hours after preparation (Supporting Information Figure S3D), makes it likely thatleakage or disintegration occurred during gel mixing rather than during freeze-drying.

It has been previously shown that the dispersion of liposomes (lecithin shell) in a collagen gel enhancedtheir chemical stability but decreasedtheir permeability.[42]A similar stabilization effect was also observed by Shi et al [43] and Mady[44]. This effect was ascribed to the collagen capacity to interact with the liposomal surface and/or to the polymer insertion in the particle membrane.[44]Likewise, the apparent phospholipid/surfactant shell destabilization of LNP could beattributed to thecollagen presence. Thus, in spite of some loss during the first 10 days after gel preparation, theFRET signalremained stable for up to23 days inthe F120 sample and for 105 days in the F50 sample, indicating that a significant fraction of LNP infreeze-dried collagen scaffoldsretainedtheir DiI/DiDcontent during long term storage.

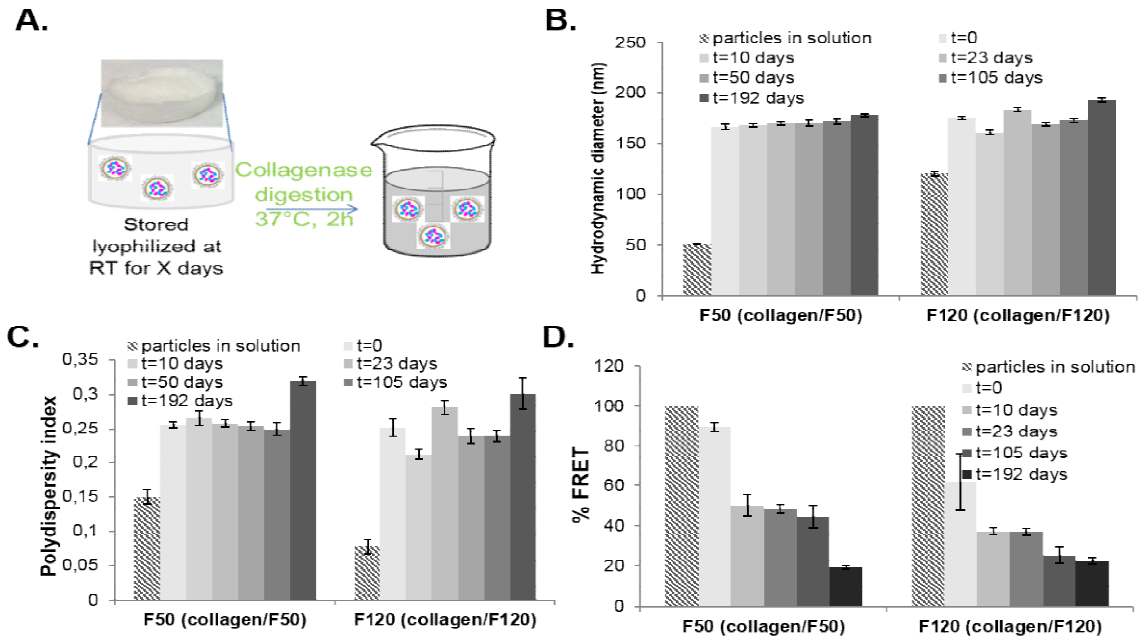

Figure 3. Stability of lipid nanoparticles embedded in cryostructurates.To monitor their stability during ambient storage, particles were extracted from collagen cryostructurates by collagenase digestion (**A**), and characterized by DLS (hydrodynamic diameter (**B**) and polydispersity index (**C**)) and measurement of FRET ratio (**D**).

2.3 Structure of collagen fibers

Native collagen is an organized structure comprised of tightly interwoven fibers resulting from the self-assembly of tropocollagen(3peptide chains arranged in a triple helix conformation). Due to the staggered arrangement of the constituting polypeptides, collagen fibers exhibit a distinctive banding pattern (D-band, spaced about 67 nm).[45]Collagen can be structurally altered by either chemical cross-linking or biomedical handling. An example is provided by the introduction of carbon nanotubes in collagen gels that elongated the D-band pattern.[46]Given this possibility, the ultrastructure of collagen/lipid nanoparticle cryostructurateswas further explored by TEM (**Figure 4**) and AFM(**Figure 5**). Under these conditions, collagen cryostructurates appeared comprised of filamentous and laminar structures made of compact fibrils exhibiting the typical banding patterns of native collagens. At the TEM level, nanoparticles appearedas spherical structures uniformlydispersed amidstcollagen fibers (**Figures 4 A,B**). No nanoparticles could be envisioned in control

collagen gels (Figure 4C) as well as in gels mixed with the Myrj™s40 co-surfactant prior to freeze-drying (Figure 4D). The expected rangeof the nanoparticle sizes (50 nm or 120 nm diameter, Figure 4)was also confirmed by image analysis. However, when observed by AFM, nanoparticles appeared as facetted nanostructures in the form of aggregates or attached to collagen fibers,and slightly larger than lipid particles(Figure 5A, 5B).

The particle facetted aspect and their size increase could be due to a process of lipid crystallization, even though thiscould not be demonstratedby DSC analysis in aqueous solutions.[36]Lipid crystallization could also be due toLNP interacting with collagen fibers or, more probably,tothe spin coating of the collagen/LNP film on silicon substrate. Interestingly, D-band spacing pattern of collagen/LNP samples was not significantly modified, indicating thatcollagen fiberswere well preserved in the presence of nanoparticles (Figure 5D).The overall structural organization of thesecollagen fibers could be maintained for nanoparticle concentration up to a collagen/lipid ratio of 2/1 (Supporting Information Figure S5), while it became more relaxed for collagen/lipid ratios below 2.5/1.

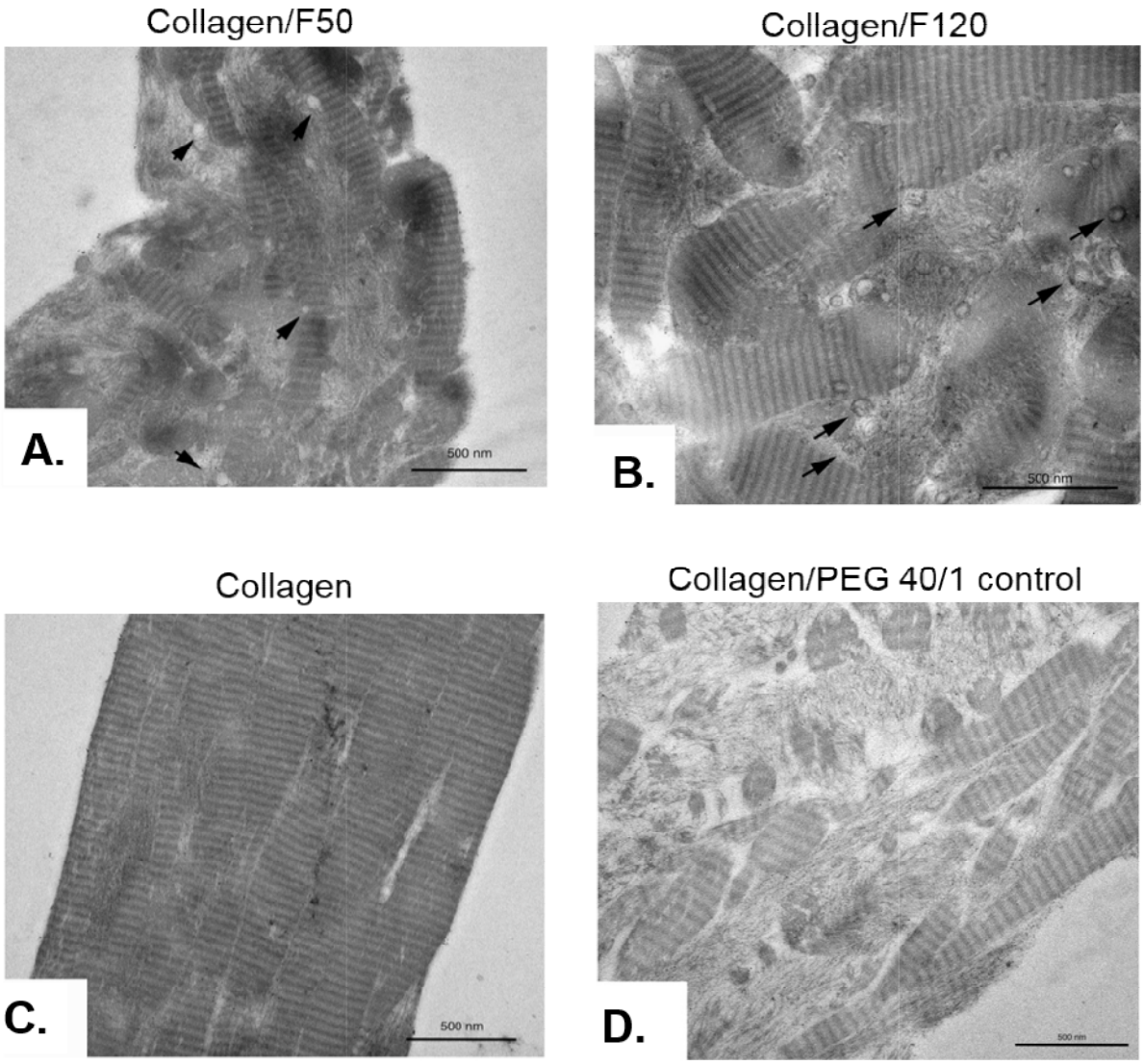

Figure 4. TEM analysis of sections of collagen cryostructurates(scale bars: 500 nm).

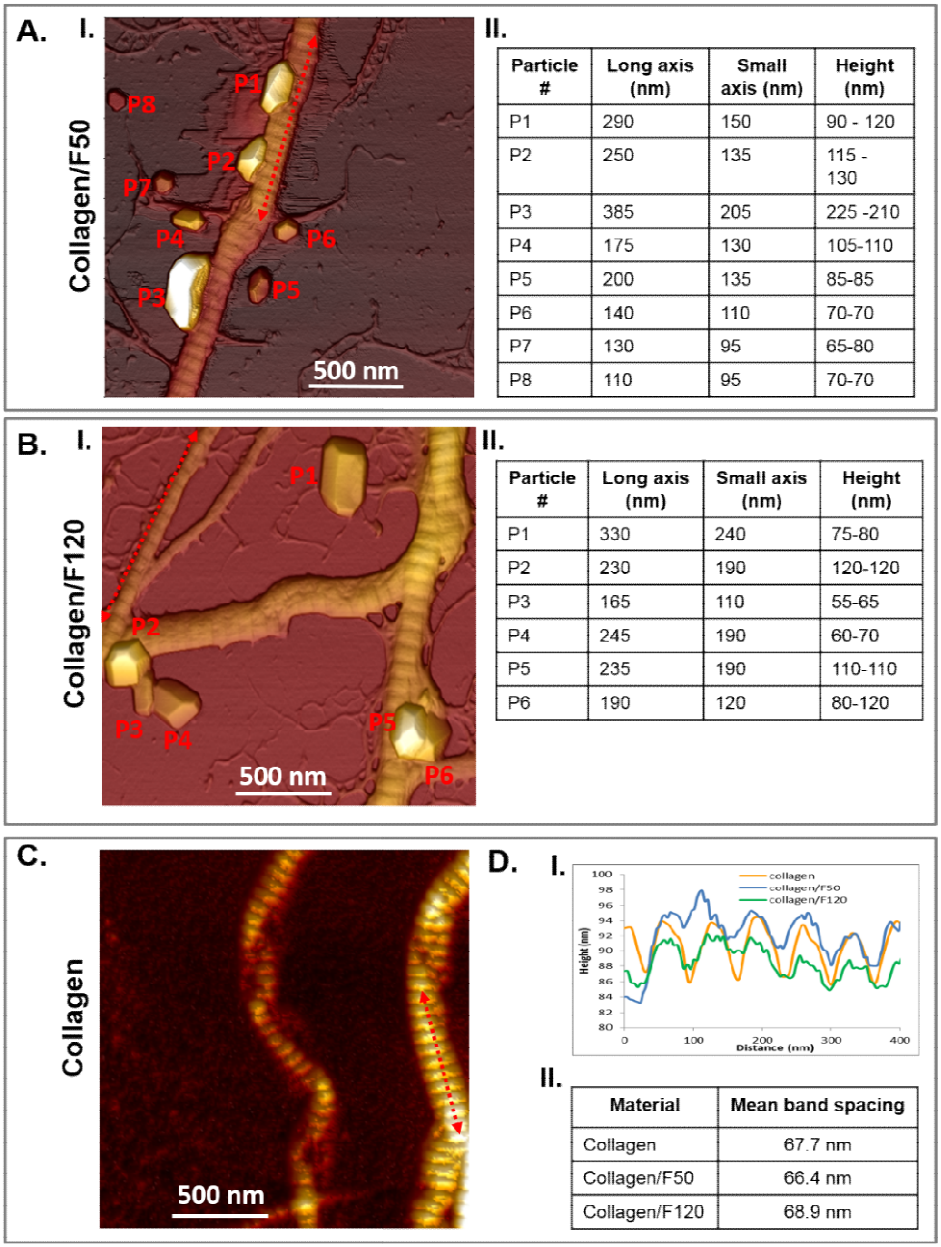

Particle #	Long axis (nm)	Small axis (nm)	Height (nm)
P1	290	150	90 - 120
P2	250	135	115 - 130
P3	385	205	225 -210
P4	175	130	105-110
P5	200	135	85-85
P6	140	110	70-70
P7	130	95	65-80
P8	110	95	70-70

Particle #	Long axis (nm)	Small axis (nm)	Height (nm)
P1	330	240	75-80
P2	230	190	120-120
P3	165	110	55-65
P4	245	190	60-70
P5	235	190	110-110
P6	190	120	80-120

Material	Mean band spacing
Collagen	67.7 nm
Collagen/F50	66.4 nm
Collagen/F120	68.9 nm

Figure 5. AFM analysis (in air) of collagen (**C**) or collagen/lipid nanoparticle films (**A, B** : I. images; II. Particle size analysis). **D.** Band spacing analysis of the collagen fibers: I: height profile along the arrows indicated in images (AI, BI, C) and II: mean band spacing measured for different samples.

The observation that, under these conditions, the collagen ultrastructure was preserved was confirmed by determiningitsthermal stability with Differential Scanning Calorimetry (DSC).[47] Data are summarized in Table 1 and plots are displayed in Figure S6 of Supporting Information. The shrinkage temperature was determined as the onset value of the endothermic peak and the thermal denaturation temperature (for helix-to-coil transition of the collagen

fibers) was taken at the endothermic peak maximum. The value of denaturation enthalpy was calculated with respect to the weight of dried collagen. Particle coating did not affect the collagen structure,as indicated by the observation that it did notimpactthe thermal denaturation temperature ofboth collagen/F50 and collagen/F120 samples (Table 1). However, particle coating augmented significantlyits shrinkage temperature (>+3°C), suggesting a potential protective role. Higher denaturation enthalpies were also observed for collagen/F50 and collagen/F120 samples, in line with the expectation thatthe fiber helical structure was protected when coated with lipid nanoparticles. The thermal stabilizing effect of LNP was, however, lowerthan that measured incross-linked collagen.[6, 47]

Table 1. Physico-chemical parameters of the collagen cryostructurates.

Material	**Structural characterization (SEM)**	**Thermal Characterization (DSC)**			**Mechanical characterization**	**Swelling ratio (SR)**
	Pore Feret's diameter [µm]	Shrinkage temperature (onset) [°C]	Thermal denaturation temperature (peak) [°C]	Denaturation enthalpy [J/g]	E* [kPa]	SR in 1X PBS
Collagen	87 ± 58	49.8	59.3	42.9	111.4 ± 6.2	5.28 ± 0.16
Collagen/F50	99 ± 62	53.6	60.1	53.2	73.3 ± 31.0	5.22 ± 0.22
Collagen/F120	98 ± 60	55.3	59.3	58.4	57.1 ± 3.0	5.02 ± 0.25

2.4. Mechanical properties, swelling ratio and particle release

Collagen/lipid cryostructurates appeared qualitatively softer (i.e. more deformable under compression) than pure collagen materials. Compression experiments were therefore performed to assess the mechanical properties of the cryostructurates and stress-strain curves are displayed in Supporting Information Figure S7.The stress-strain plots obtained were typical of elastic foam-like materials,[48] and the elastic moduli E* of the scaffolds were calculated as the slopes of stress-strain curves for very low strains (linear domain,

deformation < 3%) (Table 1). E* were in the range of previously reported values for non-crosslinked equine collagen I scaffolds,[47-48] and were indeed lower for the collagen/LNP scaffolds in comparison to pure collagen cryostructurates, with a more pronounced effect for collagen/F120 than for collagen/F50. This is indicative that LNP did not act as rigidifying matrix cross-links as observedfor other nanoparticle types, such as gold nanoparticles[49] or cellulose nanocrystals.[50]

The gel absorbing capacity was also quantified by measuring its swelling ratio in 1X PBS(10 mM phosphate, 0.137 M NaCl, pH 7.4). Data show that, in line with other observations,[47]collagen gels took up ≈ 5 folds their weight of water (Table 1). However, slightly lower swelling ratios could be observed in the presence of lipid nanoparticles, and more so for the F120 than for the F50 sample, perhaps in response to the hydrophobic effect exerted by nanoparticle coating. Overall, thesecryostructuratesexhibited very good absorbing properties under conditions that are typical of the biological fluids released during wound healing. These swelling properties, along with the cryostructuratemicroporosity,should favor nanoparticlediffusion outside the scaffolds.However, the double encapsulation strategy has been shown to prolong the kinetics of drug release from the collagen hydrogels. For instance,gentamicinewas released in about 10 days from collagen/PLGA microparticle hybrid cryostructurates,while the free drug diffused out ofcollagen material in 2 hours.[12]

Given these alternatives, the release of DiI/DiDfluorescent dyes(i.e. in or out the lipid nanoparticles)from collagen/LNPscaffolds was studied for collagen/F50 and collagen/F120cryostructuratesusing fluorescence and FRET quantification(**Figure 6A**). Results show that both dyes diffusedout ofthe collagen cryostructuratesquite slowly, displayingtwo different phases. In the first “burst release” phase, about 30% of the F50-loaded dye and 20% of the F120-loaded dyewere released in 2 days. As indicated by DLS and FRET measurement on gel supernatants, at this stage LNP were still intact and unchanged in

sizes (Supporting Information Figure S8). In a second “prolonged release” phase, dyes escaped more slowly and achieved a complete release within 25 days. It thus appears that, in the time lapse from day 14 to 25, dyes were released partly in the form of encapsulated particles and partly as free molecules (Supporting Information Figure S8). Similar diffusion patterns have been reported for other lipid nanoparticle/hydrogels (in particular polysaccharide-based) by us [51] and others[52].

Lipid nanoparticle diffusion from hydrogels is a diffusion-driven process.[52] The first “burst release” phase could be accounted for by the fast diffusion of LNP directly contacting the water phase, whereas deeper particles would take longer to escape.[51] Apparently, diffusion is more influenced by charge and hydrogel pore size than by particle size.[51-52] Indeed, as observed here, the diffusion kinetics of F50 was only a bit faster than that of F120 nanoparticles (Figure 6A).

The study of drug/particle diffusion in PBS buffer provides good comparative indications for understanding the kinetics of drug delivery. However, the wound exudate is known to contain proteases that induce drug release throughcollagen digestion. Since native collagen is known to be quickly degraded in the presence of bodily fluids, the adoption of cross-linking strategies is generally pursued to prolong itslifetime.[4]The kinetics of collagen degradation was thus assessedby titrating the 4-hydroxyproline content in the presence of collagenase (1U/mg) **(Figure 6B)**. Under these conditions, three days of incubation sufficedto degrade collagen completely,native collagen and collagen/lipid nanoparticle cryostructuratesexhibiting similar degradation kinetics. In this experiment, the presence of lipid nanoparticles did not prevent collagen degradation, while chondroitin sulfate-loaded liposomes have been previously reported to decrease collagen biodegradability in hydrogels.[37] This difference may be accounted for by the steric hindrance exerted by liposomes at collagenase cleavage sites. However, liposome loading decreased significantly the porosity,while increased pore

size, of the collagen scaffold [37](Figure 2, Table 1). These latter considerations make collagen interactions with the LNP quite different from those observed with liposomes. Overall, collagen/LNP cryostructuratescould be reasonably counted amongst the most efficient wound dressings, displaying such remarkable features as high mechanical strength, high porosity,satisfactory swelling ratiosand a prolonged drug release.

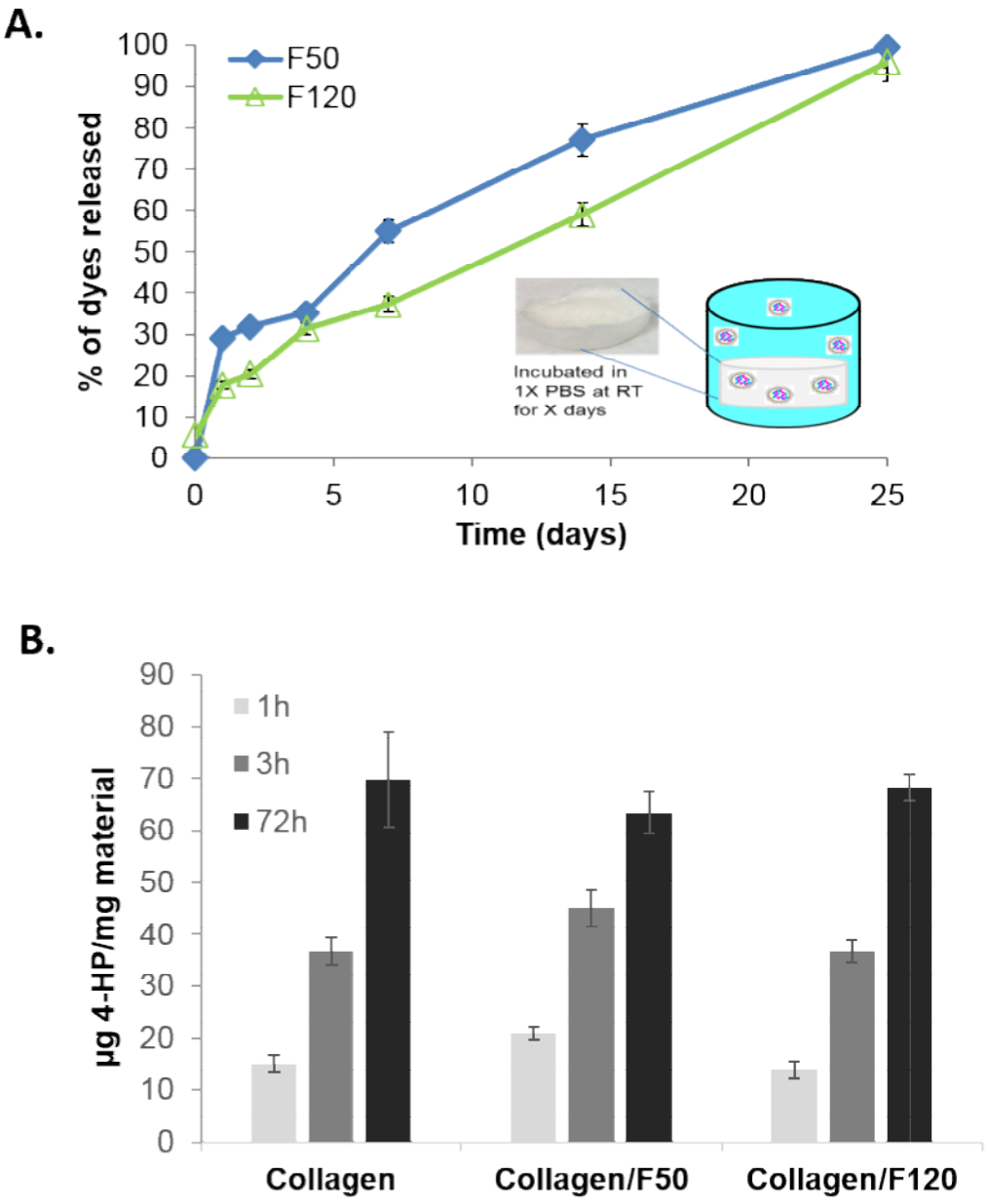

Figure 6. Kinetics of dye release from collagen/lipid cryostructurates immersed in 1X PBS buffer**(A)** and collagenbiodegradability in presence of collagenase **(B)**.

2.5 Cell proliferation and interaction with cryostructurates

Collagen is known to play key rolesin cell adhesion, migration and differentiation, dueto the presence of RGD integrin recognition sequences.[4] Therefore, to verify how collagen/LNP cryostructuratesaccomplish these functions their interactionswith fibroblasts and keratinocytes was studied*in vitro*. To this end, NIH 3T3 fibroblasts were seeded on cryostructurates(collagen, collagen/F50, collagen/F120) contained in 35 mm Petri dish in a $2x10^5$ cells/matrix ratio.Cell proliferation was monitored by measuring the mitochondrial enzyme succinate dehydrogenase activity (MTT assay). MTT activity started to increase48 hours after seedingboth in collagen and cryostructurates loaded with 10% w/w lipid nanoparticles (Supporting Information **Figure S9**).SEM and TEM images of cryostructuratesexposed to NIH 3T3 fibroblasts for 4 hours or 3 days are presented in **Figure 7**. Four hours after seeding (Figure 7A), cells appeared firmly anchored onboth collagen and collagen/LNPcryostructuratesthrough the extension of several filopodia(Figure 7 A.II). At the ultrastructural level, several contact points could be envisioned between fibroblasts and collagen/F50 fibers (Figure 7A.V), which also included intact 50 nm particles (arrows) adhering ontosome collagen fibers and other fibrillar material (Figure 7A.V). Figure 7A.VI shows a NIH 3T3 fibroblast of the collagen/F120 sample with an incorporated collagen fiber.

The extent of cell interaction increased with prolonged culturing times (Figure 7B), conferringa more relaxed aspect to the collagen fibres (Figures 7B.I and IV). By comparison, fibres of the collagen/F50 (Figures 7B.II and V) and collagen/F120 (Figures 7B.III and VI) samples remained more compact, making visiblesome of the 50 nm (Figure 7B.V) or 120 nm (Figure 7B.VI) nanoparticles. At this incubation time, NIH 3T3 fibroblasts of the collagen/F50 sample appeared to have incorporated some collagen fibres (Figure 7B Figure

7C). Figure 7C-I shows cytoplasmic protrusions enveloping collagen fibres and F50 nanoparticles, while Figure 7C-II shows a nanoparticle in contact with the cell membrane.

Similar experiments were conductedusingHaCat keratinocytes seeded on collagen cryostructuratesat the $2x10^5$ cells/matrix ratio. Three days of *in vitro* culturing sufficed to show that cells proliferatequite well regardless of the collagen matrices(Supporting Information, Figure S9). However, whilecollagen/F50 and collagen/F120 samplescouldstill exhibit some intact fibers after either 3 days (Figure S10) or 7 days (Figure S11), control collagen matrix was completely degraded.

In conclusion, both collagen/F50 and collagen/F120cryostructuratesdisplayed good adhesion properties for both keratinocytes and fibroblasts. Apparently, the porosity and mechanical strengthprovided by these scaffolds were suitable for cells to migrate and adhere on the collagen matrix. As well known, native collagen is a MMP substrate. In the absence of any MMP-inhibiting activity, as in certain chronic wounds, the metalloproteinase level is not properly regulated,[4] and collagen is consequently quickly degraded. As a result, collagen peptide fragments lose any binding activity for sequestering inflammatory mediators.[3-4]In the attempt to overcome this difficulty cross-linked collagens have been used, though soon substituted by native collagen when applied onto a wound.[3]In the present study, we proved that fibres of the collagen/LNP cryostructurateswere more resistant to enzymatic degradation than pure collagen (Figures 7 and S10-S11). The observation that LNP maintaineda fibrillary structure in collagen cryostructurates could be of high interest for designing slow degrading non-cross-linked scaffolds for prolonged application at the wound site. In addition, the observation that fibroblasts and keratinocytes incorporated collagen suggest the possibility that the associate nanoparticles could be used as potential toolsdeliveringspecific payloadstothe cells involved in wound healing (Figure 7C).

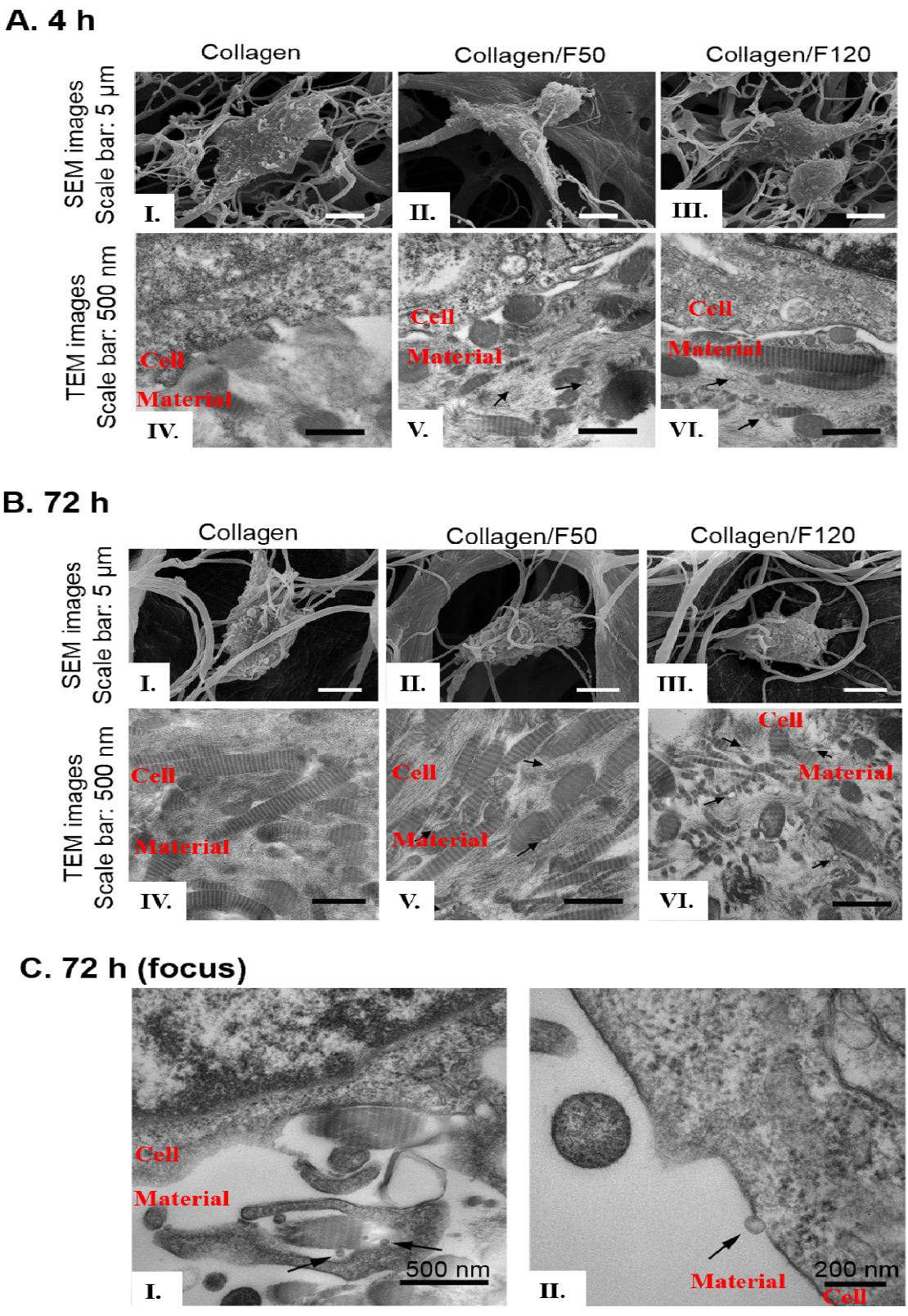

Figure 7. NIH 3T3 fibroblast/collagen cryostructurate interactions assessed by SEM and TEM 4 hours (**A**) and 3 days (**B,C**) after cell seeding.(**C**) TEM images focusing on points of interaction between a NIH 3T3 cell and collagen/F50 cryostructurates 3 days after seeding. Nanoparticles are indicated by arrows.

3. Conclusion

The ideal biomaterial promoting wound healing should display different features.[4] First, it should attract cells capable of restoring new tissues. Collagen has been shown to be a biomaterial of choice to achieve this goal for its high biocompatibility, non-immunogenicity and for expressing a large number of RGD integrin-binding sites. Second, it should promote cell proliferation, modulate proteolytic activity and guide the organization of new ECM. Chronic wounds develop whenever MMPs overexpression results in excessive matrix degradation.[3-4]

In this study, we demonstratedthat curcumin-loaded collagen cryostructuratescame to express these desirable features when recast by double encapsulation technology. Curcumin-loaded nanoparticles did not significantly modify such structural properties as high porosity, swelling ratio, matrix degradability and cell interactions, indicating thatthey entertainedonly feeble interactions and no cross-links with the collagen fibers. Even thoughnanoparticles entrapment made the collagen cryostructurates softer than controls, cryostructurates proved capable of maintaining excellent integrity when soaked in buffered saline. Thanks to the double encapsulation strategy, curcumin was released rather slowly from the scaffold, with the potential benefit for a prolonged therapeutic effect. There were also preliminary indications that fiber coating by LNP could slow down their degradation rate and prolong their structural persistence. Overall, curcumin-loaded collagen/lipid nanoparticle cryostructuratespromised to provide innovative scaffolds for treating chronic wounds.

4. Experimental Section

Materials: Gel of 1% w/w collagen type I extracted from equine Achilles tendon in acetic acid pH 3 was kindly provided by Euroresearch. Briefly, tendons were removed of all surrounding tissues, harvested and cleaned in deionized water. They were then treated with

10% sodium chloride at 4°C for 24 h under continuous magnetic stirring. The mixture was centrifuged and the precipitated collagen fibers repeatedly washed and eventually recovered with a 0.5% *w/v* solution of acetic acid.[10]Curcumin (> 97%) was purchased from TCI Europe N.V. (Paris, France), Suppocire NB™ from Gattefossé (Saint-Priest, France), Lipoid S75 (soybean lecithin at >75% phosphatidylcholine) from Lipoid (Ludwigshafen, Germany), Myrj™ S40 (polyethylene glycol 40 stearate) and super refined soybean oil from CrodaUniqema (Chocques, France), 1,1'-Dioctadecyl-3,3,3',3'-tetramethylindocarbocyanine perchlorate (DiI) and 1,1'-dioctadecyl-3,3,3',3'-tetramethylindotricarbocyanine perchlorate (DiD) from LifeTechnologies (Saint-Aubin, France). Other chemicals were purchased from Sigma-Aldrich (Saint-Quentin-Fallavier, France).

*Nanoparticle synthesis and characterization:*Lipid nanoparticles of different diameters (50 nm: F50, 120 nm: F120) were prepared according to previously described protocols.[34]Briefly, an oily mixture composed of soybean oil (85 mg/150 mg, respectively for F50/F120), Suppocire NB™ (255 mg/450 mg respectively) and Lipoid-s75® (65 mg/45mg respectively), added with curcumin (7.5 mg/8.6 mg respectively) or dyes (DiI or/and DiD), supplied in ethanol, was mixed with an aqueous phase composed of Myrj™ S40 (stearate-PEG_{40}, 345 mg/215 mg respectively) in 10 mM phosphate buffer pH 7.4 (1X PBS, 1250 µL/1140 µL respectively). Sonication cycles were performed at 45°C for 5 minutes to yield particle dispersion with the desired hydrodynamic diameter. LNP were protected from light and dialyzed overnight in 1X PBS (10 mM phosphate, 0.137 M NaCl, pH 7.4)at room temperature. Samples were diluted to obtain a concentration of 100 mg/ml of lipids (including soybean oil, Suppocire NB™, lecithin and Myrj™ S40). LNPwere then sterilized by filtration using 0.22 µm filters, stored at 4°C and light proof. Dynamic light scattering (DLS) was usedtodetermineparticlehydrodynamicdiameterandzeta potential (ZetaSizer Nano ZS,

Malvern Instrument). Particlesweredilutedto 2 mg/mloflipids in sterile 0.1X PBS (1 mMphosphate, 13.7 mM NaCl, pH 7.4) andtransferred in ZetaSizer Nano cells (Malvern Instrument) beforeeachmeasurement, performed in triplicate. Curcuminencapsulationyield was determinedby HPLC analysis after particledestabilization in acetonitrile. Chromatographicanalysis was achieved on a C18 column (Sunfire™, 5 mm, 250 4.6 mm, 100 Å) using an Alliance 2695 separationmoduleequippedwith a controller 600 and a 2487 Dual AbsorbanceDetectorset at 265 and 420 nm (Waters, USA), and data were processed using Empower 2 software. Theelution methodusedabinarygradientmobilephaseconsistingof(A)a mixtureofwateracidifiedwith2%(v/v)acetic acidand(B)acetonitrile, at a 1 ml/min flow rate.Thegradientwas appliedasfollowing:0–12minfrom60to100%B;12–17min from100%to60%B;17–20min60%B.

*Collagen cryostructurate preparation:*25 g of collagen gel at 1% w/w in acetic acid buffer (containing 250 mg of collagen) were mixed with the appropriate volume of F50 or F120 at 100 mg/ml for 1 hour at room temperature (20°C).2 g of gel material were distributed into each well of 12 well cell culture plates. The upper surface was covered with a polypropylene membrane before freezing in liquid nitrogen for 5 min. The freeze-drying process was done for 24 hours with a Cryotec V8.11 plate lyophilizer. Control collagen/Myrj™ s40 (collagen/PEG) materials were prepared at the40/1 w/wratio. Collagen cryostructurates directly loaded with curcumin were prepared using the same procedure by mixing 25 g of collagen gel with 250 µg of curcumin dissolved in 250 µl of ethanol.

*Particle stability when embedded in the collagen cryostructurates:*Nanoparticles were extracted from cryostructurate to determine their stability during storage.1 ml of collagenase

solution (1.5 mg/ml collagenase, 1 mg/ml $CaCl_2$ in 1X PBS) was added to 4 mg of lyophilized collagen and incubated at 37°C for 3 hours. Undigested materials, precipitated calcium chloride and collagenase were eliminated by centrifugation at 10,000 g for 2 minutes. The supernatant, containing digested collagen and nanoparticles, was analyzed by DLS measurements (particle colloidal stability) and by fluorescence spectroscopy using a Perkin-Elmer LS50B fluorimeter (DiI and DiD co-localization reflects the LNP integrity, as assessed by the DiD/DiI fluorescence ratio[41]). FRET data were expressed as % of FRET, calculated as:% FRET=100 × [(DiD)/Dil (t)- DiD⁄Dil (100% dissociation))/(DiD/Dil (fresh solution)-DiD⁄Dil (100% dissociation)]**.** The DiD/DiI fluorescence ratio at 100% dissociation was obtained by incubating nanoparticles in DMSO toyield to their total destruction in a few minutes.

*Scanning Electron Microscopy:*Collagen scaffoldswere cut with a sterile razor blade into a number of small blocks and attached to aluminum stubs with a carbon tape. Blocks were oriented to expose either the upper or the lower surface, while others were glued on their longitudinal cut profile. For SEM analysis, collagen/lipid particle cryostructuratesand their cellular loads were cut into a number of small blocks with a sterile razor blade and fixed overnight with 3% glutaraldehyde at 4 °C in phosphate buffer (PB) at pH 7.2. Following extensive rinsing with the same buffer at 4 °C, they were immersed for 1h in 0.5% tannic acid in PB at 4 °C, rinsed again four times in the same buffer for 15 min at 4 °C, and eventually post-fixed for 1h with 1% osmium tetroxide in PB at 4 °C. Specimens were finally washed in distilled water, block-stained with 1% uranyl acetate in distilled water and then dehydrated in a graded series of ethanols. Samples were first dried by the critical point method in a Balzers Union CPD 020 and then sputter-coated with gold in a Balzers MED 010 unit to be observed in a JEOL JSM 6010LA electron microscope.

*Transmission Electron Microscopy:*Collagen/lipid particle cryostructurateswere cut into a number of small blocks with a sterile razor blade and fixed as specified above. Following dehydration in a graded series of ethanol, samples were infiltrated for two days in graded mixtures of LRWhite resin/ethanol. By the end of this procedure, samples were embedded in fresh LRWhite resin and cut with Reichert Ultracutultramicrotome equipped with a diamond knife. Ultrathin sections (60-80 nm thick) were collected on copper grids, stained with uranyl acetate and lead citrate, and observed with a JEOL 1200 EX II electron microscope. Micrographs were acquired by the Olympus SIS VELETA CCD camera equipped the iTEM software.

Atomic Force Microscopy: Collagen/LNP films were deposited and dried on SiO_2 substrates by spin coating for AFM observation in air. We used PeakForce Tapping on a Dimension ICON microscope (Bruker) with a "ScanAsyst Air" tip (Bruker). The stiffness of each tip (k ~0.4 N/m) was obtained by thermal noise method after photodiode calibration on a hard and rigid substrate (Al_2O_3). Images were acquired with an average setpoint force of ~ 500 pN. Scan speed was set and adapted during imaging to obtain an average error on force feedback less or equal of 10% of the force setpoint value.

*Differential Scanning Calorimetry:*33-45 mg dry collagenweresoaked for 1h in deionized water, dried on filter paper for 1 minute, weighted again and sealed in aluminum pans. DSC analysis was carried out on a micro DSC III SETARAM calorimeter. An aluminum pan with the same weight of deionized water was used as a reference. Heating rate was set at a constant value of 3°C/min and the temperature increased from 20 °C to 110°C. Several duplicates (2 to 5) of the same sample (from different batches) were analyzed.

*Uniaxial compression test:*Uniaxial compression tests were performed on lyophilized cylinder shaped collagenof 4.1 mm diameter and 5 mm height using an AR2000EX rheometer (TA instrument) with an initial preload of 0.03 N and a compression speed of 10 µm/s. Stressσ was calculated as the normal force divided by the collagen surface area, whereas strainε was expressed as the percentage of collagen compression.

*Swelling ratio:*Collagen scaffolds were cut in small pieces (about 1 cm x 1 cm), weighed and soaked for 24 hours in 5 ml of phosphate-buffered saline (PBS) buffer, at room temperature (20°C). Non-absorbed solution was removed by aspiration andwet materials dried for 3 minutes on a filter paper. Finally, wet collagen samples were weighed and their swelling ratio (SR) calculated according to the following equation:$SR = (W_w - W_d) / W_d$in which W_d is the dry weight (i.e. lyophilized collagen prior to PBS soaking) and W_w is the resulting wet weight. 3 to 6 sample /point were used.

*Kinetics of release of the dyes from the collagen cryostructurates:*For each time point,5-10 mg samples were incubated at 37°C in 1 ml1X PBS. 300 µl of supernatant were then takenup and analyzed by DLS measurements (particle colloidal stability) and fluorescence spectroscopy using a Perkin-Elmer LS50B fluorimeter. Dye concentration and FRET percentagewere calculated from the fluorescence spectra, as specified above.

*Kinetics of degradation of the collagen cryostructurates:*Kinetics of the cryostructuratedegradation was measured by quantifying the 4-hydroxyproline (Hyp) released following collagenase (*Clostridium histolycum*)digestion. Five mg of each samplewere incubated at 37°C with 5 units of collagenase solution (Sigma-Aldrich C0130) diluted to 5

mlof0.01M Tris-HCl, pH 7.2, containing 50mM $CaCl_2$, for the desired time of digestion. The solution was filtered with a 5μm pore polypropylene filterto remove the degradation products. 4-Hyp concentration was determined using the Hydroxyproline Assay Kit (Sigma-Aldrich, MAK008).[53]

Cell culture: Human keratinocytes (HaCat) and stabilized murine fibroblasts (NIH 3T3) were cultured in 75 cm^2 flasks containing DMEM (Dulbecco's Modified Eagle's Medium), supplemented with 10% of newborn calf serum (NCS) and fetal bovine serum (FBS) respectively, 1% glutamine and 1% penicillin/streptomycin, and maintained in an incubator at 37 °C with 5% CO_2 and controlled humidity (cell incubation time 24 h). Upon reaching confluence, cells were passed into new culture vessels in a 1:5 ratio and the medium changed every three days.

*Cell proliferation:*Cell proliferation was assessed using the MTT assay. NIH3T3 mousefibroblasts ($2x10^5$cells/well) wereseeded in 12-well platescontaininglyophilizedcollagen (25 mg)and incubated for 24, 48 and 72 hours with 2 ml of culture medium. At each incubation time the culture medium were withdrawn and 0.2 ml MTT (Sigma-Aldrich) were added to every aliquot and left to incubate for 4 hours in the dark at 37 °C under a 5% CO_2 flow. By the end of this incubation time, the resulting formazan crystals were completely dissolved in DMSO and the relative absorbance measured at a wavelength of 570 nm.Cells culturedwithnocollagenandcellsincubatedin presence of zinc wereusedas positive and negative controls, respectively. The percentageofcellproliferation was determinedusingthefollowingequation: Cellproliferation (%) = ((AS–ANC)/(APC–ANC)×100) where AS, representthe sample absorbance; ANC, thenegative control (cellswithzinc material);andAPC, thepositive control (onlycells).

*Collagen/Cell interaction:*Cells were seeded on the top surface of lyophilized collagen scaffolds in 35 mm Petri dish, with $2x10^5$ cells/matrix. Collagens and cells were then incubated at 37°C in 2 ml of culture medium under a continuous flow of 5% CO_2. Medium was then renewed every 3 days. SEM and TEM imaging were performed as described above.

Acknowledgements

This work was supported by the EU-funded FP7 ICT- 317894 SWAN-iCare project. Valentina Laghezza Masci thanks Euroresearch for a PhD financial support. OzgülTezgel thanks the French National Research Agency (ARCANE project n° ANR-12-LABX-003) for financial support. We are grateful to Dorothée Joud and Marie Escudé for helping us in the preparation of particle batches, Mathilde Menneteau for help in cell proliferation experiments, Pierre Moscatellofor 4-hydroxyproline titration, and Lisa Racine for DSC and mechanical compression experiments. The authors acknowledge Prof. Rachel Auzély at CERMAV Grenoble France for access to the AR2000EX rheometer.

References

[1] M. Ashtikar, M. G. Wacker, *Adv. Drug Deliv. Rev.* **2018**, *129*, 194.
[2] L. N. Kasiewicz, K. A. Whitehead, *Biomater. Sci.* **2017**, *5*, 1962.
[3] S. Chattopadhyay, R. T. Raines, *Biopolymers* **2014**, *101*, 821.
[4] L. J. Gould, *Adv. Wound Care* **2016**, *5*, 19.
[5] C. A. Fleck, R. Simman, *J. Am. College Certified Wound Specialists* **2010**, *2*, 50.
[6] V. V. S. Reddy Karri, G. Kuppusamy, S. V. Talluri, S. S. Mannemala, R. Kollipara, A. D. Wadhwani, S. Mulukutla, K. R. S. Raju, R. Malayandi, *Int. J. Biol. Macromol.* **2016**, *93*, 1519.
[7] R. Parenteau-Bareil, R. Gauvin, S. Cliche, C. Gariépy, L. Germain, F. Berthod, *Acta Biomaterialia* **2011**, *7*, 3757.
[8] R. Guo, Y. Lan, W. Xue, B. Cheng, Y. Zhang, C. Wang, S. Ramakrishna, *J.Tissue Eng. Regen. Med.* **2017**, *11*, 3544.
[9] J. C. Karr, A. R. Taddei, S. Picchietti, G. Gambellini, A. M. Fausto, F. Giorgi, *Adv. in Skin Wound Care* **2011**, *24*, 208.
[10] V. Laghezza Masci, A. R. Taddei, G. Gambellini, F. Giorgi, A. M. Fausto, *J. Biomed. Mat. Res. A* **2016**, *104*, 272.
[11] V. Laghezza Masci, A. R. Taddei, G. Gambellini, F. Giorgi, A. M. Fausto, *J. Circulating Biomarkers* **2016**, *5*, 1849454416663660.
[12] Z. Ruszczak, W. Friess, *Adv. Drug Deliv. Rev.* **2003**, *55*, 1679.
[13] J. S. Boateng, K. H. Matthews, H. N. E. Stevens, G. M. Eccleston, *J. Pharm. Sci.* **2008**, *97*, 2892.
[14] D. Kumar, M. Kumar, C. Saravan, S. K. Singh, *Expert Opin. Ther. Targets* **2012**, *16*, 959.
[15] P. Tyagi, M. Singh, H. Kumari, A. Kumari, K. Mukhopadhyay, *PLoS ONE* **2015**, *10*, e0121313.
[16] V. Kant, A. Gopal, D. Kumar, N. N. Pathak, M. Ram, B. L. Jangir, S. K. Tandan, D. Kumar, *J. Surg. Res.* **2015**, *193*, 978.
[17] Y.-H. Yen, C.-M. Pu, C.-W. Liu, Y.-C. Chen, Y.-C. Chen, C.-J. Liang, J.-H. Hsieh, H.-F. Huang, Y.-L. Chen, *Int. Wound J.* **2018**, *15*, 605.
[18] C. Mohanty, S. K. Sahoo, *Drug Discov.Today* **2017**, *22*, 1582.
[19] M. Alibolandi, M. Mohammadi, S. M. Taghdisi, K. Abnous, M. Ramezani, *Int. J. Pharm.* **2017**, *532*, 466.
[20] L. H. Dang, T. H. Nguyen, H. L. B. Tran, V. N. Doan, N. Q. Tran, *J. Healthcare Eng.* **2018**, *2018*, 14.
[21] X. Li, S. Chen, B. Zhang, M. Li, K. Diao, Z. Zhang, J. Li, Y. Xu, X. Wang, H. Chen, *Int. J. Pharm.* **2012**, *437*, 110.
[22] Y.-H. Lin, J.-H. Lin, Y.-S. Hong, *J. Biomed. Mater. Res. B* **2017**,*105*, 81.
[23] M. C. Teixeira, C. Carbone, E. B. Souto, *Prog. Lipid Res.* **2017**, *68*, 1.
[24] R. H. Müller, R. Shegokar, C. M. Keck, *Curr. Drug Discover.Technol.* **2011**, *8*, 207.
[25] R. H. Müller, M. Radtke, S. A. Wissing, *Adv. Drug Deliv. Rev.* **2002**, *54*, S131.
[26] L. B. Jensen, K. Petersson, H. M. Nielsen, *Eur. J. Pharm. Biopharm.* **2011**, *79*, 68.
[27] N. B. Wolf, S. Küchler, M. R. Radowski, T. Blasschke, K. D. Kramer, G. Weindl, B. Kleuser, R. Haag, M. Schäfer-Korting, *Eur. J. Pharm. Biopharm.* **2009**, *73*, 34.
[28] X. Chen, L.-H. Peng, Y.-H. Shan, N. Li, W. Wei, L. Yu, Q.-M. Li, W.-Q. Liang, J.-Q. Gao, *Int. J. Pharm.* **2013**, *447*, 171.
[29] I. Garcia-Orue, G. Gainza, C. Girbau, R. Alonso, J. J. Aguirre, J. L. Pedraz, M. Igartua, R. M. Hernandez, *Eur. J. Pharm. Biopharm.* **2016**, *108*, 310.

[30] G. Gainza, W. S. Chu, R. H. Guy, J. L. Pedraz, R. M. Hernandez, B. Delgado-Charro, M. Igartua, *Int. J. Pharm.* **2015**, *490*, 404.
[31] C. R. Cardoso, S. Favoreto Jr, L. L. Oliveira, J. O. Vancim, G. B. Barban, D. B. Ferraz, J. S. Silva, *Immunobiol.* **2011**, *216*, 409.
[32] L. M. Pereira, E. Hatanaka, E. F. Martins, F. Oliveira, E. A. Liberti, S. H. Farsky, R. Curi, *Cell Biochem. Func.* **2008**, *26*, 197.
[33] Y. Yamaguchi, T. Nagasawa, A. Kitagawa, N. Nakamura, K. Matsumoto, H. Uchiwa, K. Hirata, R. Igarashi, *Parmazie* **2006**, *61*, 112.
[34] J. Gravier, F. Navarro, T. Delmas, F. Mittler, A. C. Couffin, F. Vinet, I. Texier, *J. Biomed. Opt.* **2011**, *16*, 096013.
[35] F. P. Navarro, G. Creusat, C. Frochot, A. Moussaron, M. Verhille, R. Vanderesse, J.-S. Thomann, P. Boisseau, I. Texier, A.-C. Couffin, M. Barberi-Heyob, *J. Photochem. Photobiol. B* **2014**, *130*, 161.
[36] T. Delmas, A. C. Couffin, P. A. Bayle, F. d. Crécy, E. Neumann, F. Vinet, M. Bardet, J. Bibette, I. Texier, *J. Colloid Interf. Sci.* **2011**, *360*, 471.
[37] O. Craciunescu, A. Gaspar, M. Trif, M. Moisei, A. Oancea, L. Moldovan, O. Zarnescu, *J. Nanomater.* **2014**, *2014*, 9.
[38] C. J. Doillon, C. F. Whyne, S. N. Brandwein, F. H. Silver, *J. Biomed. Mater. Res.* **1986**, *20*, 1219.
[39] G. S. Offedu, J. C. Ashworth, R. E. Cameron, M. L. Oyen, *J. Mechan. Behavior Med. Mater.* **2015**, *41*, 19.
[40] B. J. Lawrence, S. V. Madihally, *Cell Adhesion Migration* **2008**, *2*, 9.
[41] J. Gravier, L. Sancey, S. Hirsjärvi, E. Rustique, C. Passirani, J. P. Benoit, J. L. Coll, I. Texier, *Mol. Pharm.* **2014**, *11*, 3133.
[42] M. Pajean, D. Herbage, *Int. J. Pharm.* **1993**, *91*, 209.
[43] X. Shi, W. Ma, C. Sun, S. Wu, *Biomater.* **2001**, *22*, 1627.
[44] M. M. Mady, *J. Biosci. Bioengin.* **2007**, *104*, 144.
[45] S. Zhu, Q. Yuan, T. Yin, J. You, Z. Gu, S. Xiong, Y. Hu, *J. Mater. Chem. B* **2018**, *6*, 2650.
[46] T. Kim, I. Sridharan, B. Zhu, J. Orgel, R. Wang, *Mater. Sci. Eng. C* **2015**, *49*, 281.
[47] P. Angele, J. Abke, R. Kujat, H. Faltermeier, D. Schumann, M. Nerlich, B. Kinner, C. Englert, Z. Ruszczak, R. Mehrl, R. Mueller, *Biomater.* **2004**, *25*, 2831.
[48] B. A. Harley, J. H. Leung, E. C. C. M. Silvo, L. Gibson, *Acta Biomaterialia* **2007**, *3*, 463.
[49] T. Schuetz, N. Richmond, M. E. Harmon, J. Schuetz, L. Castaneda, K. Slowinska, *Colloids Surf.B* **2013**, *101*, 118.
[50] W. Li, R. Guo, Y. Lan, Y. Zhang, W. Xue, Y. Zhang, *J. Biomed. Mat. Res. A* **2014**, *102*, 1131.
[51] L. Racine, A. Guliyeva, I. Wang, V. Larreta-Garde, R. Auzély-Velty, I. Texier, *Macromol. Biosci.* **2017**, *17*, 1700045.
[52] C. Desfrançois, R. Auzely, I. Texier, *Pharm.* **2018**, *accepted*.
[53] G. Kesava Reddy, C. S. Enwemeka, *Clin. Biochem.* **1996**, *29*, 225.